

## Article

# Precision Higgs Constraints in $U(1)$ Extensions of the Standard Model with a Light $Z'$ -Boson

Zoltán Péli <sup>1</sup>  and Zoltán Trócsányi <sup>1,2,\*</sup> 

<sup>1</sup> Institute for Theoretical Physics, ELTE Eötvös Loránd University, Pázmány Péter Sétány 1/A, 1117 Budapest, Hungary; zoltan.peli@ttk.elte.hu

<sup>2</sup> HUN-REN ELTE Theoretical Physics Research Group, Pázmány Péter Sétány 1/A, 1117 Budapest, Hungary

\* Correspondence: zoltan.trocsanyi@cern.ch

**Abstract:** Anomaly-free  $U(1)$  extensions of the standard model (SM) predict a new neutral gauge boson  $Z'$ . When  $Z'$  obtains its mass from the spontaneous breaking of the new  $U(1)$  symmetry by a new complex scalar field, the model also predicts a second real scalar  $s$ , and the search for the new scalar and the search for the new gauge boson become intertwined. We present the computation of production cross sections and decay widths of such a scalar  $s$  in models with a light  $Z'$  boson when the decay  $h \rightarrow Z'Z'$  may have a sizeable branching ratio. We show how the Higgs signal strength measurement in this channel can provide stricter exclusion bounds on the parameters of the model than those obtained from the total signal strength for Higgs boson production.

**Keywords:** beyond the standard model; superweak extension; new neutral gauge boson; scalar search; exclusion limits

## 1. Introduction

While the discovery of the Higgs boson [1,2] has established the existence of a scalar elementary particle, the thorough understanding of the role of scalar fields in nature remains elusive. So far all experimental results are in agreement with the structure of the scalar sector of the standard model (SM) [3], although the scalar potential has not yet been fully confirmed experimentally, which allows for the existence of an extended scalar sector. Indeed, there is a vigorous experimental search for new scalar particles at the LHC [4]. The more complex such an extended sector, the more new particles should exist and the more difficult the search strategies.

The  $U(1)$  extensions of the SM have the potential to explain several beyond the standard model (BSM) phenomena at the cost of predicting the existence of  $Z'$ , a new neutral gauge boson. In the simplest scenario,  $Z'$  acquires its mass from the spontaneous breaking of a new scalar field  $\chi$  [5]; hence, the model also predicts a new scalar particle  $s$ .  $Z'$  bosons appear in a wide variety of models; for a comprehensive review on them, see Ref. [6]. Experiments searched extensively for new scalar particles, as well as a new  $Z'$  boson (for an incomplete list, we refer to Refs. [7–10]). In such  $U(1)$  extensions, the existence of  $s$  and  $Z'$  are interconnected. For instance, if  $Z'$  is sufficiently light, then the Higgs boson and the new scalar can decay into a  $Z'$  pair as shown on Figure 1. The channel  $h \rightarrow Z'Z'$  can significantly alter the decay properties of the Higgs boson, which consequently can be used to constrain the free parameters of the model.



Academic Editors: Wolfgang Schafer and Roman Pasechnik

Received: 22 November 2024

Revised: 16 December 2024

Accepted: 19 December 2024

Published: 3 January 2025

**Citation:** Péli, Z.; Trócsányi, Z. Precision Higgs Constraints in  $U(1)$  Extensions of the Standard Model with a Light  $Z'$ -Boson. *Universe* **2025**, *11*, 12. <https://doi.org/10.3390/universe11010012>

**Copyright:** © 2025 by the authors. Licensee MDPI, Basel, Switzerland. This article is an open access article distributed under the terms and conditions of the Creative Commons Attribution (CC BY) license (<https://creativecommons.org/licenses/by/4.0/>).

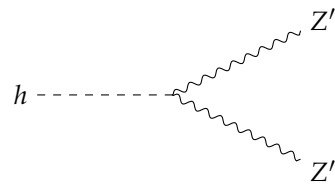


**Figure 1.** Tree-level diagram of the Higgs boson decaying into two  $Z'$  bosons.

An example of such a simple  $U(1)$  extension of the standard model, with the potential to explain all established experimental observations that cannot be interpreted within the SM, is the superweak extension of the standard model (SWSM) [11]. It is designed to explain (i) the non-vanishing masses of neutrinos, (ii) the nature of dark matter, (iii) the origin of baryon asymmetry, and (iv) the role of scalar fields in the universe.

The SWSM extends the gauge group of the SM  $G = SU(3)_c \otimes SU(2)_L \otimes U(1)_Y$ , to  $G \otimes U(1)_z$ . The corresponding neutral gauge field becomes massive by introducing a complex scalar field  $\chi$  with a non-zero vacuum expectation value (VEV). The gauge and gravity anomalies are required to cancel, which is achieved by introducing three generations of right-handed neutrinos—dubbed heavy neutral lepton (HNL), below—with properly chosen  $z$  charges  $z_N$ . If we also allow the presence of Dirac-type Yukawa terms for the HNLs, then two independent  $z$  charges remain. We choose the  $z$  charge  $z_\phi$  of the Brout–Englert–Higgs (BEH) field and  $z_N$  to be the free, model-dependent parameters. All new fields are neutral under the standard model gauge interactions. The SWSM fixes the  $z$  charge of the BEH field to  $z_\phi = 1$ , and those of the HNLs to  $z_N = \frac{1}{2}$  by allowing also the Majorana-type Yukawa term in the Lagrangian for the HNLs and normalizing the new gauge coupling  $g_z$  such that the new scalar has  $z$  charge  $z_\chi = -1$ .

In this work, we compute benchmark points for the production and decay of a new scalar  $s$  for models with a light  $Z'$  boson. If the  $Z'$  is light, the decay  $h \rightarrow Z'Z'$  may have a sizeable branching ratio with dominant contribution independent of  $z_\phi$  and  $z_N$ . We show that exclusion limits on new singlet scalar particles obtained from signal strength measurements can be improved by taking into account the process  $h \rightarrow Z'Z'$ . We provide a *Mathematica* notebook that can be used flexibly to compute benchmark points relevant for scalar searches at the LHC. While the specific model we have in mind is the SWSM, our analysis is valid for an arbitrary assignment of  $z$  charges.

Experiments often search for the so-called dark photon, which appears in the  $U(1)$  extensions with  $z_\phi = z_N = 0$ . These results can be translated to  $U(1)$  extensions with arbitrary  $z$  charge assignment [12]. The prospects of discovering a dark photon were studied extensively [13] by also taking into account the channels  $h \rightarrow ZZ'$  and  $h \rightarrow Z'Z'$ . Our approach is different in the sense that we investigate the prospects of discovering a new scalar  $s$  when the model also predicts a  $Z'$  boson with unconstrained  $z_\phi$  and  $z_N$  charges.

## 2. Scalar Sector of the SWSM

In this section, we collect the details of the model only to the extent used in the present analyses.

In the scalar sector, in addition to the  $SU(2)_L$ -doublet Brout–Englert–Higgs field,

$$\phi = \begin{pmatrix} \phi^+ \\ \phi^0 \end{pmatrix} = \frac{1}{\sqrt{2}} \begin{pmatrix} \phi_1 + i\phi_2 \\ \phi_3 + i\phi_4 \end{pmatrix}, \tag{1}$$

the model contains a complex scalar SM singlet  $\chi$ . The Lagrangian of the scalar fields contains the potential energy

$$V(\phi, \chi) = -\mu_\phi^2 |\phi|^2 - \mu_\chi^2 |\chi|^2 + (|\phi|^2, |\chi|^2) \begin{pmatrix} \lambda_\phi & \frac{\lambda}{2} \\ \frac{\lambda}{2} & \lambda_\chi \end{pmatrix} \begin{pmatrix} |\phi|^2 \\ |\chi|^2 \end{pmatrix} \subset -\mathcal{L} \quad (2)$$

where  $|\phi|^2 = |\phi^+|^2 + |\phi^0|^2$ . After spontaneous symmetry breaking, we parametrize the scalar fields as

$$\phi = \frac{1}{\sqrt{2}} \begin{pmatrix} -i\sqrt{2}\sigma^+ \\ v + h' + i\sigma_\phi \end{pmatrix}, \quad \chi = \frac{1}{\sqrt{2}}(w + s' + i\sigma_\chi) \quad (3)$$

where  $v$  and  $w$  are the vacuum expectation values of  $\phi$  and  $\chi$ . The fields  $h'$  and  $s'$  are real scalars,  $\sigma^+$  is charged, and  $\sigma_\phi$  and  $\sigma_\chi$  are neutral Goldstone bosons that are gauge eigenstates.

The gauge and mass eigenstates are related by the rotations

$$\begin{pmatrix} h \\ s \end{pmatrix} = \mathbf{Z}_S \begin{pmatrix} h' \\ s' \end{pmatrix}, \quad \begin{pmatrix} \sigma_Z \\ \sigma_{Z'} \end{pmatrix} = \mathbf{Z}_G \begin{pmatrix} \sigma_\phi \\ \sigma_\chi \end{pmatrix}, \quad (4)$$

with

$$\mathbf{Z}_X = \begin{pmatrix} \cos \theta_X & -\sin \theta_X \\ \sin \theta_X & \cos \theta_X \end{pmatrix} \quad (5)$$

where we denote the mass eigenstates with  $h, s$  and  $\sigma_Z, \sigma_{Z'}$ . The angles  $\theta_S$  and  $\theta_G$  are the scalar and Goldstone mixing angles that can be determined by the diagonalization of the mass matrix of the real scalars and that of the neutral Goldstone bosons. In the following, we use the abbreviations  $c_X = \cos \theta_X$  and  $s_X = \sin \theta_X$  for the mixing angles.

### Scalar Couplings

The vertices that involve the scalars are related to the corresponding vertices in the SM by simple proportionality factors involving the scalar mixing angle  $\theta_S$ . Hence, if possible, we present the Feynman rules expressed using the corresponding SM rule.

- Scalar–fermion couplings:

$$\Gamma_{hff} = c_S \Gamma_{hff}^{\text{SM}}, \quad \Gamma_{sff} = s_S \Gamma_{hff}^{\text{SM}}. \quad (6)$$

- Scalar–vector boson couplings:  $i\Gamma_{SVV}g^{\mu\nu}$  where

$$\Gamma_{hWW} = c_S \Gamma_{hWW}^{\text{SM}}, \quad \Gamma_{sWW} = s_S \Gamma_{hWW}^{\text{SM}} \quad (7)$$

and

$$\begin{aligned} \Gamma_{hZZ} &= 2M_Z^2 \left( c_S c_Z^2 - \frac{s_S}{\tan \beta} s_Z^2 \right), & \Gamma_{sZZ} &= 2M_Z^2 \left( s_S c_Z^2 + \frac{c_S}{\tan \beta} s_Z^2 \right), \\ \Gamma_{hZZ'} &= 2M_Z M_{Z'} s_Z c_Z \left( c_S + \frac{s_S}{\tan \beta} \right), & \Gamma_{sZZ'} &= 2M_Z M_{Z'} s_Z c_Z \left( s_S - \frac{c_S}{\tan \beta} \right), \\ \Gamma_{hZ'Z'} &= 2M_{Z'}^2 \left( c_S s_Z^2 - \frac{s_S}{\tan \beta} c_Z^2 \right), & \Gamma_{sZ'Z'} &= 2M_{Z'}^2 \left( s_S s_Z^2 + \frac{c_S}{\tan \beta} c_Z^2 \right) \end{aligned} \quad (8)$$

where  $\tan \beta = w/v$  is the ratio of the VEVs. In the SWSM region of the parameter space, the neutral boson mixing angle  $\theta_Z$  is smaller than  $\mathcal{O}(10^{-3})$  [14]; hence, we consider the leading contributions to the vertex factors  $\Gamma_{SVV}$  in the limit  $\theta_Z \rightarrow 0$  ( $c_Z = 1, s_Z = 0$ ).

- Scalar–scalar couplings:

$$\begin{aligned} \Gamma_{hss} &= + \frac{M_H^2 + 2M_s^2}{v} s_S c_S \left( \frac{c_S}{\tan \beta} - s_S \right), \\ \Gamma_{shh} &= - \frac{2M_H^2 + M_s^2}{v} s_S c_S \left( \frac{s_S}{\tan \beta} + c_S \right). \end{aligned} \tag{9}$$

In these vertex factors the replacement  $h \rightarrow s$  can be achieved by ( $c_S \rightarrow s_S, s_S \rightarrow -c_S$ ) and the replacement of one  $Z \rightarrow Z'$  by *one factor* of ( $c_Z \rightarrow s_Z, s_Z \rightarrow -c_Z$ ). Thus, it is sufficient to define explicitly  $\Gamma_{hZZ}$  and  $\Gamma_{hss}$ .

### 3. Production of Scalar Particles in the LHC

The production cross sections of a scalar particle that mixes with the SM scalar, which we shall refer to as *Higgs-like new scalar*, can be computed based on Ref. [15]. There are several production channels for the Higgs boson at the LHC, and similarly for the new scalar as well. These channels involve (i) gluon-gluon fusion (ggF), (ii) associated production of the scalar with a vector boson (VS), (iii) vector boson fusion (VBF), and (iv) associated production of the scalar with a  $t\bar{t}$  pair (ttS).

In the SWSM, the new scalar is directly coupled to heavy quarks, so the dominant production channel is the gluon–gluon fusion as in the SM. The difference compared to the  $\Gamma_{hff}$  vertex is only a proportionality factor obtained from the scalar mixing angle  $\theta_S$  given in Equation (6), and hence, the gluon fusion cross sections for the production of the two scalar particles are proportional:

$$\sigma(gg \rightarrow h) = c_S^2 \sigma^{\text{SM}}(gg \rightarrow h), \quad \sigma(gg \rightarrow s) = s_S^2 \sigma^{\text{SM}}(gg \rightarrow h)|_{M_h \rightarrow M_s}. \tag{10}$$

The associated production of the scalar boson with a vector boson  $V$  involves the couplings (8) between the scalars and the vector bosons, which provide factors of  $c_S^2$  and  $s_S^2$  as compared to the SM. In addition, there is a contribution due to the  $SZ'$  channel, but it is negligibly small compared to the  $SW$  or  $SZ$  channels for small  $Z'$  masses,  $\xi = M_{Z'}/M_Z \ll 1$ , relevant in the SWSM parameter space. The V-A couplings of the  $Z$  boson to the quarks also receives BSM corrections, but these are well measured quantities, and the deviation from the SM must be small. Hence, the  $Vh$  production cross section receives only an overall factor  $c_S^2$  as compared to the SM model prediction:

$$\sigma(pp \rightarrow Vh) = c_S^2 \sigma^{\text{SM}}(pp \rightarrow Vh). \tag{11}$$

Thus, measuring  $\sigma(pp \rightarrow Vh)$  and comparing it to the SM prediction for this process constrains  $c_S$ .

By far the most complicated process to compute its cross section is the vector boson fusion. However, the radiative corrections are known to be small [15], so we consider this channel only at the leading order (LO) in perturbation theory. The partonic process is  $qq \rightarrow qq + (V^*V^* \rightarrow h)$ . The squared matrix element of this process at LO is proportional to  $G_F^3 M_V^8$ , which means that the VBF process is also heavily suppressed when  $V = Z'$  and  $\xi \ll 1$ . Thus, only  $V = Z$  and  $W$  contribute with suppression factors  $c_S^2$  for the Higgs production and  $s_S^2$  for the new Higgs-like scalar production:

$$\sigma(qq \rightarrow qqh) = c_S^2 \sigma^{\text{SM}}(qq \rightarrow qqh), \quad \sigma(qq \rightarrow qq_s) = s_S^2 \sigma^{\text{SM}}(qq \rightarrow qqh)|_{M_h \rightarrow M_s}. \tag{12}$$

The scalar boson can also be produced in association with heavy quarks. This has the smallest contribution to the total production rate even when the heavy quark is the  $t$ -quark. The Higgs-like new scalar is directly coupled to heavy quarks just like in the Higgs

boson, and the suppression factor in the production cross section is  $\tan^2(\theta_S)$  just like in gluon–gluon fusion:

$$\sigma(pp \rightarrow t\bar{t}s) = s_S^2 \sigma^{\text{SM}}(pp \rightarrow t\bar{t}h)|_{M_h \rightarrow M_s}. \tag{13}$$

Based on its small contribution to the total production cross section, we neglect this production channel in our analysis.

We see that all important production cross sections are proportional to the cross section of the Higgs boson production in the SM with the relevant scalar mass value. Then, it is sufficient to precisely compute the Higgs boson production cross section for different values of the Higgs mass. One can use automated software for that purpose, or alternatively, one can save data using plots from Ref. [16], which we do here to obtain the relevant  $K$ -factors.

## 4. Decays of Scalars

### 4.1. Total Width of the Higgs Boson

The SM theoretical prediction for the Higgs boson width is  $\Gamma_h^{\text{SM}} = 4.07$  MeV, with a relative uncertainty of 4% [3]. The experimental measurements on the other hand are  $\Gamma_h^{\text{ATLAS}} = 4.5^{+3.3}_{-2.5}$  MeV [17] and  $\Gamma_h^{\text{CMS}} = 3.2^{+2.4}_{-1.7}$  MeV [18], displaying a much larger uncertainty than the SM theoretical prediction, allowing for several BSM models to remain compatible with observations.

In the superweak and other  $U(1)_z$  extensions with a light  $Z'$  boson ( $M_{Z'} \ll M_Z$ ), the decay  $h \rightarrow Z'Z'$  is allowed with partial width

$$\Gamma(h \rightarrow Z'Z') = \frac{G_F M_h^3}{16\sqrt{2}\pi} \left( \frac{s_S}{\tan \beta} \right)^2 + \mathcal{O}\left(\frac{M_{Z'}^2}{M_Z^2}\right), \tag{14}$$

and the total width of the Higgs boson is

$$\Gamma_h = c_S^2 \Gamma_h^{\text{SM}} + \Gamma(h \rightarrow Z'Z'), \tag{15}$$

which can be used to constrain the parameters  $\theta_S$  and  $\tan \beta$ . We see that the total decay width can be smaller in the extended model than that in the SM depending on the relative effect of the scalar mixing angle and the partial decay width of the Higgs boson into the new neutral gauge boson pair.

### 4.2. Decay Channels

A Higgs-like new scalar has similar decay channels to the Higgs boson as listed.

**Fermionic:** The decays into SM fermions are only affected by an overall factor of  $s_S^2$  as compared to the SM. If the mass of the Higgs-like scalar is above the  $2m_N$  threshold, it can also decay into a pair of HNLs, with partial width

$$\Gamma(S \rightarrow N_i N_i) = \frac{G_f M_s m_{N_i}^2}{8\sqrt{2}\pi} \left( 1 - \frac{4m_{N_i}^2}{M_s^2} \right)^{3/2} \left( \frac{c_S}{\tan \beta} \right)^2. \tag{16}$$

The Higgs boson can also decay into an HNL pair, provided the process is allowed kinematically. The corresponding partial decay width can be obtained from Formula (16) with the replacements  $M_s \rightarrow M_h$  and  $c_S \rightarrow s_S$ .

**Loop induced:** This category includes the decays into  $\gamma\gamma$ ,  $gg$  and  $Z\gamma$  as well as  $Z'\gamma$ . In the important decay channels  $s \rightarrow \gamma\gamma$  and  $gg$ , the decay widths are only multiplied by an overall  $s_S^2$  factor,

$$\Gamma(s \rightarrow \gamma\gamma, Z\gamma, gg) = s_5^2 \Gamma^{\text{SM}}(h \rightarrow \gamma\gamma, Z\gamma, gg)|_{M_h \rightarrow M_s}. \tag{17}$$

The  $Z'\gamma$  channel is also interesting because the LHC cast exclusion limits specifically on this channel (with branching ratio  $\text{Br}(Z'\gamma) < 2\%$ ), but the prediction for this branching fraction is much smaller than the experimental limit. In the case of a light  $Z'$  and a modest  $Z - Z'$  mixing, its contributions are negligibly small.

**Decays into a pair of heavy vector bosons:** The decays of the Higgs-like scalar into a charged  $W$ -pair is only affected by an overall factor of  $s_5^2$  as compared to the SM prediction. Decays into heavy neutral bosons are controlled by the  $SZ^{(\prime)}Z^{(\prime)}$  vertex. The vertex  $SZZ'$  is naturally suppressed, but the  $SZ'Z'$  may be large.

**Decays into scalars:** In the case of  $M_s > 2M_h$ , the channel  $s \rightarrow hh$  opens up, while the opposite decay  $h \rightarrow ss$  is excluded by the results for  $\Gamma_h^{\text{exp}}$  compared to the SM prediction.

The decay properties of a Higgs-like new scalar depend on all free parameters of the model. An indirect restriction on the parameter space can be derived from the experimental constraints on the Higgs boson width  $\Gamma_h$ .

A more refined analysis reveals that for  $\xi \ll 1$ , such as the case of the SWSM, the free parameters reduce to a set of four parameters [19]:

$$M_s, s_5, \tan\beta, \text{ and } m_{N_i}, \tag{18}$$

where  $\tan\beta$  absorbs the free parameters of the gauge sector in the combination

$$\tan\beta \propto \frac{M_{Z'}}{|s_Z|M_Z}. \tag{19}$$

The exact formula contains an additional factor depending on the  $z$ -charge of the BEH field and the kinetic mixing between the  $U(1)$  gauge fields [14], which is not important in our analysis. We note that for the B-L  $U(1)$  extension, the proportionality factor is zero, so the scalar and gauge sector parameters are not related in that model.

### 5. Implementation

We compute the Higgs boson production cross section  $\sigma(pp \rightarrow h + X)$  at  $\sqrt{s} = 13.6$  TeV center-of-mass energies in proton–proton collisions for several values of  $M_h$  in the range [100 GeV, 1 TeV]. Producing a Higgs-like scalar means that this cross section is multiplied with  $s_5^2$ . In principle, the  $Z'$  boson affects these production rates in a nontrivial way, but these effects are negligibly small for  $M_{Z'} \ll M_Z$ , which is relevant for the SWSM.

We use the NNPDF3.0 set for the parton density functions (PDF), the LO set for LO predictions and the NLO set for the computations at the next-to-leading-order (NLO) accuracy. We use the running strong coupling from the chosen PDF set. We take the values of the other input parameters  $m_b^{\text{pole}}, m_t^{\text{pole}}, G_f, M_Z$  and  $M_W$  from Ref. [3].

We compute the production cross section from the ggF process at NLO QCD with NNLO QCD and NLO EW corrections included as a K-factor. The Vh process is implemented at NLO QCD, and finally we compute the VBF at LO, as the NLO corrections are known to be small with  $K_{\text{NLO}}^{\text{VBF}} \sim 1.1$ .

We include a *Mathematica* notebook `sWSM_scalar.nb` which contains a precomputed set of the scalar boson production cross sections and precisely computes the decay rates of the Higgs boson and the Higgs-like scalar.

### 6. Signal Strengths

If a light neutral vector boson  $Z'$  exists, the Higgs boson can decay into a  $Z'Z'$  pair, which affects the signal strengths in other channels. The signal strength measured at the LHC is

$$\mu_{\text{exp.}} = \frac{(\sigma \text{ Br})_{\text{obs}}}{(\sigma \text{ Br})_{\text{SM}}}, \tag{20}$$

while the theoretical value in the presence of new physics is

$$\mu_{\text{th.}} = \frac{(\sigma \text{ Br})_{\text{BSM}}}{(\sigma \text{ Br})_{\text{SM}}} \tag{21}$$

where the BSM subscript refers to the prediction in the full BSM model, including the SM contributions. The most precisely measured channel is  $h \rightarrow ZZ^*$  [3]. In the superweak model and in general when the Higgs boson cannot decay into an  $ss$  or HNL pair, the predicted signal strength in the  $ZZ$  channel is

$$\mu_{ZZ} = \frac{c_S^4 \Gamma_h^{\text{SM}}}{c_S^2 \Gamma_h^{\text{SM}} + \Gamma(h \rightarrow Z'Z')} \tag{22}$$

because  $\sigma_h^{\text{SWSM}} = c_S^2 \sigma_h^{\text{SM}}$  and  $\Gamma^{\text{SWSM}}(h \rightarrow ZZ) = c_S^2 \Gamma^{\text{SM}}(h \rightarrow ZZ)$ . Using the PDG24 [3] values ( $\Gamma_h \simeq 0.00407 \text{ GeV}$ ,  $M_h \simeq 125 \text{ GeV}$ ), we obtain

$$\mu_{ZZ} = \frac{c_S^4}{c_S^2 + 78.74 (s_S / \tan \beta)^2}, \tag{23}$$

which approaches  $c_S^2$  for large values of  $\tan \beta$ . In that case, the total signal strength provides a considerably more severe limit. The latter sums over all production and decay channels; hence

$$\mu_{\text{tot}} = \frac{\sigma_h^{\text{BSM}}}{\sigma_h^{\text{SM}}} = c_S^2, \tag{24}$$

in which case the experimental values are [20,21]

$$\mu_{\text{tot}}^{\text{ATLAS}} = 1.05 \pm 0.06, \quad \mu_{\text{tot}}^{\text{CMS}} = 1.02 \pm 0.06. \tag{25}$$

Then, the total signal strength yields the bounds independent of  $\tan \beta$

$$\theta_{S,\text{tot}}^{\text{ATL}} = 0.27, \quad \theta_{S,\text{tot}}^{\text{CMS}} = 0.32. \tag{26}$$

### 7. Benchmarks and Exclusion Bounds

For sufficiently small values of  $\tan \beta$ , the bound obtained from  $\mu_{ZZ}$  tends to be more constraining than that obtained from  $\mu_{\text{tot}}$ . The experimentally measured values for the  $ZZ^*$  signal strength are [20,21]

$$\mu_{ZZ}^{\text{ATLAS}} = 1.04 \pm 0.09, \quad \mu_{ZZ}^{\text{CMS}} = 0.97 \pm 0.12, \tag{27}$$

which includes all the productions channels. Figure 2 shows the limits obtained from the total signal strength measurements as well as those from the  $ZZ^*$  channel for  $\tan \beta \leq 20$ . The colored region on the  $s_S - \tan \beta$  plane is excluded at the 95% confidence level (C.L.).



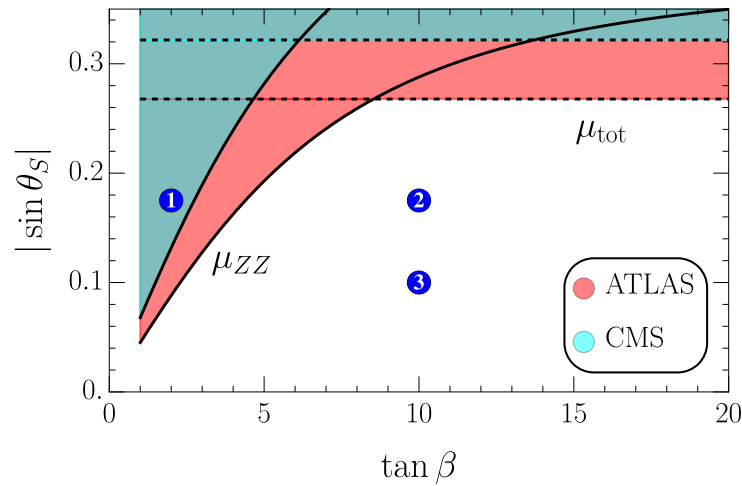


**Figure 2.** Limit on the sine of the scalar mixing angle  $\theta_S$  as a function of  $\tan \beta$ . The red (cyan) region is excluded at 95% C.L. by the ATLAS (CMS) measurement of the total and  $h \rightarrow ZZ^*$  signal strengths. The blue disks with numbers  $i$  correspond to benchmark points  $BP_i$ .

The blue discs with numbers  $i$  correspond to the benchmark points  $BP_i$  we propose based on the exclusion bounds obtained from the signal strength measurements. Explicitly, the three benchmark points are

$$\begin{aligned} BP1 : \theta_S &= 0.175, \tan \beta = 2, M_S = 500 \text{ GeV}, \\ BP2 : \theta_S &= 0.175, \tan \beta = 10, M_S = 500 \text{ GeV}, \\ BP3 : \theta_S &= 0.10, \tan \beta = 10, M_S = 1000 \text{ GeV}. \end{aligned} \quad (28)$$

where  $BP1$  is allowed by  $\mu_{\text{tot}}$  but excluded by  $\mu_{ZZ}$ , while  $BP2$  and  $BP3$  are still allowed.  $BP1$  is chosen such that finding a scalar corresponding to  $BP1$  would exclude a large class of BSM models predicting a light  $Z'$  boson. Using Equation (19), the gauge sector parameters are

$$\begin{aligned} BP1 : M_{Z'} &= 18 \text{ MeV}, \quad s_Z = 10^{-4}, \\ BP2 : M_{Z'} &= 91 \text{ MeV}, \quad s_Z = 10^{-4}, \\ BP3 : M_{Z'} &= 91 \text{ MeV}, \quad s_Z = 10^{-4}. \end{aligned} \quad (29)$$

The Higgs-portal coupling  $\lambda$  can be expressed via the relation

$$\lambda = \frac{M_S^2 - M_H^2}{v^2} \frac{s_S c_S}{\tan \beta}, \quad (30)$$

yielding

$$\lambda_{BP1} = 0.33, \quad \lambda_{BP2} = 0.07 \quad \text{and} \quad \lambda_{BP3} = 0.16. \quad (31)$$

The SWSM model contains three families HNLs  $N_i$ . We consider the masses of these particles  $M_{N_1} = \mathcal{O}(M_{Z'})$  and  $M_{N_2} = M_{N_3} = 100 \text{ GeV}$  for all benchmark points. Then, the HNLs do not contribute to the decays of the Higgs boson, and can explain dark matter abundance [22]. We present the production cross sections and branching ratios corresponding to  $BP1$ ,  $BP2$ , and  $BP3$  in Table 1. Further points can be obtained similarly using the *Mathematica* code attached.



**Table 1.** The production cross sections and branching fractions corresponding to the benchmark points defined in Equation (28).

–	<i>h</i>			<i>s</i>		
	BP1	BP2	BP3	BP1	BP2	BP3
$\sigma_{\text{prod}}$ [pb]	53	53	54	0.16	0.16	0.001
$\Gamma$ [GeV]	$6.4 \times 10^{-3}$	$4.0 \times 10^{-3}$	$4.0 \times 10^{-3}$	8.3	2.9	8.5
$\text{Br}(hh)$	–	–	–	0.09	0.23	0.20
$\text{Br}(W^+W^-)$	0.13	0.21	0.21	0.13	0.37	0.37
ine $\text{Br}(ZZ)$	0.016	0.026	0.026	0.06	0.18	0.18
$\text{Br}(Z'Z')$	0.38	0.024	0.008	0.6	0.07	0.19
$\text{Br}(b\bar{b})$	0.36	0.57	0.58	$<10^{-4}$	$<10^{-4}$	$<10^{-4}$
$\text{Br}(t\bar{t})$	–	–	–	0.05	0.14	0.05
$2 \times \text{Br}(NN)$	–	–	–	0.07	0.009	0.07

## 8. Summary

In our analysis, we focused on  $U(1)$  extensions of the SM, where the new gauge boson becomes massive via the spontaneous breaking of the new  $U(1)$  symmetry by a complex scalar field, such as in the superweak extension of the SM. We have shown that in the case of a light  $Z'$ , the new decay channel  $h \rightarrow Z'Z'$  alters the signal strengths in all decay channels of the Higgs boson. Here, we focused on the  $ZZ^*$  channel, which is measured experimentally with high precision. We obtained bounds on the free parameters of the model: the Higgs–new scalar mixing angle  $\theta_S$  and the ratio  $\tan \beta$  of the VeV of the new scalar to that of the BEH field. We presented three benchmark points: one (BP1) already excluded by the signal strength measurement in the  $ZZ^*$  decay channel of the Higgs boson, and two other ones (BP2, BP3) that are still allowed. Finding a new scalar  $s$  corresponding to BP1 would mean that no new light  $Z'$  boson exists, as it would violate the exclusion bound derived from the effect of the decay  $h \rightarrow Z'Z'$ . Further benchmark points can be generated easily using the *Mathematica* notebook as supplementary material.

**Supplementary Materials:** The following supporting information can be downloaded at: <https://www.mdpi.com/article/10.3390/universe11010012/s1>, Mathematica notebook S1: swsm\_scalar.nb.

**Author Contributions:** Conceptualization, Z.P. and Z.T.; methodology, Z.P. and Z.T.; software, Z.P.; validation, Z.P., formal analysis, Z.P.; writing—original draft preparation, Z.P.; writing—review and editing, Z.T.; visualization, Z.P.; supervision, Z.T.; project administration, Z.T.; funding acquisition, Z.P. and Z.T. All authors have read and agreed to the published version of the manuscript.

**Funding:** This research was funded by Excellence Programme of the Hungarian Ministry of Culture and Innovation grant number TKP2021-NKTA-64, by the National Research, Development and Innovation Office grant number NKFI-150794, and by the Hungarian Scientific Research Fund grant number PD-146527.

**Data Availability Statement:** All data used are included in the Supplementary Material.

**Conflicts of Interest:** The authors declare no conflicts of interest.

## Abbreviations

The following abbreviations are used in this manuscript:

SM	standard model
LHC	Large Hadron Collider
BSM	beyond the standard model
SWSM	superweak extension of the standard model
VEV	vacuum expectation value
HNL	heavy neutral lepton
BEH	Brout–Englert–Higgs
ggF	gluon–gluon fusion
VS	production of the scalar with a vector boson
VBF	vector boson fusion
ttS	production of the scalar with a $t\bar{t}$ pair
LO	leading order
NLO	next-to-leading order
NNLO	next-to-next-to-leading order
PDF	parton density function
C.L.	confidence level
BP	benchmark point

## References

1. Aad, G.; Abajyan, T.; Abbott, B.; Abdallah, J.; Abdel Khalek, S.; Abdelalim, A.A.; Abdinov, O.; Aben, R.; Abi, B.; Abolins, M.; et al. Observation of a new particle in the search for the Standard Model Higgs boson with the ATLAS detector at the LHC. *Phys. Lett.* **2012**, *B716*, 1–29. [[CrossRef](#)]
2. Chatrchyan, S.; Khachatryan, V.; Sirunyan, A.M.; Tumasyan, A.; Adam, W.; Aguilo, E.; Bergauer, T.; Dragicevic, M.; Erö, J.; Fabjan, C.; et al. Observation of a new boson at a mass of 125 GeV with the CMS experiment at the LHC. *Phys. Lett.* **2012**, *B716*, 30–61. [[CrossRef](#)]
3. Navas, S.; Amsler, C.; Gutsche, T.; Hanhart, C.; Hernández-Rey, J.J.; Lourenço, C.; Masoni, A.; Mikhasenko, M.; Mitchell, R.E.; Patrignani, C.; et al. Review of Particle Physics. *Phys. Rev. D* **2024**, *110*, 030001. [[CrossRef](#)]
4. Hayrapetyan, A.; Tumasyan, A.; Adam, W.; Andrejkovic, J.W.; Bergauer, T.; Chatterjee, S.; Damanakis, K.; Dragicevic, M.; Hussain, P.S.; Jeitler, M.; et al. Searches for Higgs boson production through decays of heavy resonances. *arXiv* **2024**, arXiv:2403.16926.
5. Appelquist, T.; Dobrescu, B.A.; Hopper, A.R. Nonexotic Neutral Gauge Bosons. *Phys. Rev. D* **2003**, *68*, 035012. [[CrossRef](#)]
6. Langacker, P. The Physics of Heavy  $Z'$  Gauge Bosons. *Rev. Mod. Phys.* **2009**, *81*, 1199–1228. [[CrossRef](#)]
7. Robens, T. Constraining extended scalar sectors at current and future colliders—An update. In Proceedings of the 8th Workshop on Theory, Phenomenology and Experiments in Flavour Physics, Capri, Italy, 11–13 June 2022; Springer: Berlin/Heidelberg, Germany, 2023; Volume 292, pp. 141–152.
8. Aad, G.; Abbott, B.; Abbott, D.C.; Abdinov, O.; Abed Abud, A.; Abeling, K.; Abhayasinghe, D.K.; Abidi, S.H.; AbouZeid, O.S.; Abraham, N.L.; et al. Search for high-mass dilepton resonances using 139 fb<sup>-1</sup> of  $pp$  collision data collected at  $\sqrt{s} = 13$  TeV with the ATLAS detector. *Phys. Lett. B* **2019**, *796*, 68–87. [[CrossRef](#)]
9. Sirunyan, A.M.; Tumasyan, A.; Adam, W.; Andrejkovic, J.W.; Bergauer, T.; Chatterjee, S.; Dragicevic, M.; Escalante Del Valle, A.; Frühwirth, R.; Jeitler, M.; et al. Search for resonant and nonresonant new phenomena in high-mass dilepton final states at  $\sqrt{s} = 13$  TeV. *JHEP* **2021**, *7*, 208.
10. Banerjee, D.; Burtsev, V.E.; Chumakov, A.G.; Cooke, D.; Crivelli, P.; Depero, E.; Dermenev, A.V.; Donskov, S.V.; Dusaev, R.R.; Enik, T.; et al. Dark matter search in missing energy events with NA64. *Phys. Rev. Lett.* **2019**, *123*, 121801. [[CrossRef](#)] [[PubMed](#)]
11. Trócsányi, Z. Super-weak force and neutrino masses. *Symmetry* **2020**, *12*, 107. [[CrossRef](#)]
12. Ilten, P.; Soreq, Y.; Williams, M.; Xue, W. Serendipity in dark photon searches. *JHEP* **2018**, *6*, 4. [[CrossRef](#)]
13. Curtin, D.; Essig, R.; Gori, S.; Shelton, J. Illuminating Dark Photons with High-Energy Colliders. *JHEP* **2015**, *2*, 157. [[CrossRef](#)]
14. Péli, Z.; Trócsányi, Z. Exclusion bounds for neutral gauge bosons. *Phys. Rev. D* **2024**, *110*, 015027. [[CrossRef](#)]
15. Djouadi, A. The Anatomy of Electro-Weak Symmetry Breaking. I: The Higgs boson in the Standard Model. *Phys. Rept.* **2008**, *457*, 1–216. [[CrossRef](#)]
16. ATLAS Wiki. Available online: <https://twiki.cern.ch/twiki/bin/view/AtlasPublic/HiggsTheoryPlots> (accessed on 18 December 2025).

17. Aad, G.; Abbott, B.; Abeling, K.; Abidi, S.H.; Aboulhorma, A.; Abramowicz, H.; Abreu, H.; Abulaiti, Y.; Abusleme Hoffman, A.C.; Acharya, B.S.; et al. Evidence of off-shell Higgs boson production from ZZ leptonic decay channels and constraints on its total width with the ATLAS detector. *Phys. Lett. B* **2023**, *846*, 138223. [[CrossRef](#)]
18. Tumasyan, A.; Adam, W.; Andrejkovic, J.W.; Bergauer, T.; Chatterjee, S.; Damanakis, K.; Dragicevic, M.; Escalante Del Valle, A.; Frühwirth, R.; Jeitler, M.; et al. Measurement of the Higgs boson width and evidence of its off-shell contributions to ZZ production. *Nat. Phys.* **2022**, *18*, 1329–1334.
19. Péli, Z.; Trócsányi, Z. Precise prediction for the mass of the W boson in gauged U(1) extensions of the standard model. *Phys. Rev. D* **2023**, *108*, L031704. [[CrossRef](#)]
20. Aad, G.; Abbott, B.; Abbott, D.C.; Abeling, K.; Abidi, S.H.; Aboulhorma, A.; Abramowicz, H.; Abreu, H.; Abulaiti, Y.; Abusleme Hoffman, A.C.; et al. A detailed map of Higgs boson interactions by the ATLAS experiment ten years after the discovery. *Nature* **2022**, *607*, 52–59; Erratum in *Nature* **2022**, *612*, E24.
21. Tumasyan, A.; Adam, W.; Andrejkovic, J.W.; Bergauer, T.; Chatterjee, S.; Damanakis, K.; Dragicevic, M.; Escalante Del Valle, A.; Hussain, P.S.; Jeitler, M.; et al. A portrait of the Higgs boson by the CMS experiment ten years after the discovery. *Nature* **2022**, *607*, 60–68; Erratum in *Nature* **2023**, *623*, E4.
22. Iwamoto, S.; Seller, K.; Trócsányi, Z. Sterile neutrino dark matter in a U(1) extension of the standard model. *JCAP* **2022**, *1*, 35. [[CrossRef](#)]

**Disclaimer/Publisher’s Note:** The statements, opinions and data contained in all publications are solely those of the individual author(s) and contributor(s) and not of MDPI and/or the editor(s). MDPI and/or the editor(s) disclaim responsibility for any injury to people or property resulting from any ideas, methods, instructions or products referred to in the content.